resection were treated with carboplatin plus either etoposide or vincristine. One patient (case 44), who had complete tumor removal, underwent combined radiotherapy and ACNU (3-[(4-amino-2-methyl-5-pyrimidinyl) methyl]-1-(chloroethyl)-1-nitrosourea) chemotherapy. At relapse, chemotherapy was used in a few cases following the same scheme.

Prognosis

Of the 44 patients, 32 were still alive. The median follow-up period for the whole population was 63.1 months. The follow-up period was longer than 4 years for 21 patients (48 %) and longer than 10 years for six (14 %). OS was 84.5 % (CI 95 %: 73.7–96.7) after 24 months and 71.6 % (CI 95 %: 55.7–92.0) after 10 years (Fig. 2a). On univariate analysis, OS was not influenced by sex, tumor size, radiotherapy, or chemotherapy, but was influenced by type of surgery (biopsy vs partial resection vs gross total resection) ($p = 0.04$) (Table 3). Older age was associated with a shorter OS ($p = 0.03$). Median PFS was 38.4 months (CI 95 %: 29.2–72.5). PFS was 68.9 % (CI 95 %: 55.6–85.2) after 24 months, 37.9 % (CI 95 %: 24.0–69.9) after 48 months, and 26.6 % (CI 95 %: 13.4–52.7) after 72 months (Fig. 2b). On univariate analysis, PFS was not influenced by age, sex, chemotherapy, or radiotherapy (Table 3). In total, 25 patients (56.8 %) experienced at least one relapse, the primary site being affected in 22. Of the 22 patients presenting with local recurrences, 13 were irradiated and nine were not. Two patients underwent radiosurgery (cases 4 and 42), 10 localized conformal radiotherapy (cases 2, 3, 7, 10, 14, 17, 27, 29, 36 and 38), and one craniospinal irradiation with a boost to the primary site (case 6). One patient had local recurrence and fourth ventricle spread (case 29). Three other patients had distant relapse, one with spinal spread (case 5), one with simultaneous spinal and meningeal spread (case 26), and one with cerebellar spread (case 35). Twelve patients experienced a second relapse, which was local in 7 cases (cases 1, 4, 6, 13, 24, 27, and 29) or extended in 5 cases: bulbar (case 2), cerebellar and frontal ventricular (case 20), spinal and entire ventricular system (case 22), local with posterior fossa extension (case 31), and cerebellar (case 35). Of the 7 cases with local recurrence, 5 had adjuvant treatments after the first surgery: radiotherapy, chemotherapy alone or with craniospinal irradiation, stereotactic radiosurgery, or brachytherapy. Five patients had a third relapse and one patient a fourth. After the second or subsequent relapses, 2 patients had chemotherapy: one (case 22) received gemcitabine–oxaliplatine (GEMOX) as second line chemotherapy for a spinal and ventricular relapse and showed a partial response after 9 cycles, while the other (case 35) showed a partial response after 9 cycles of carboplatin plus etoposide.

Discussion

The present series of 44 cases represents the largest retrospective series of PTPRs to date, extending previously published data [4] by increasing the number of patients and doubling the median follow-up period to 63.1 months. This tumor occurs across a wide age range (from 5 to 66 years in our series), with the vast majority occurring in young adults, in agreement with other reports [14–16]. Some cases have already been described in children [4, 17–19], one being a 15 month-old boy, the youngest patient to present with PTPR [18].

Radiological descriptions of PTPR are quite rare. In our series, MRI results was not always available, so a detailed review of imaging findings was not performed. Radiologically, PTPRs are mildly lobulated, partially cystic,

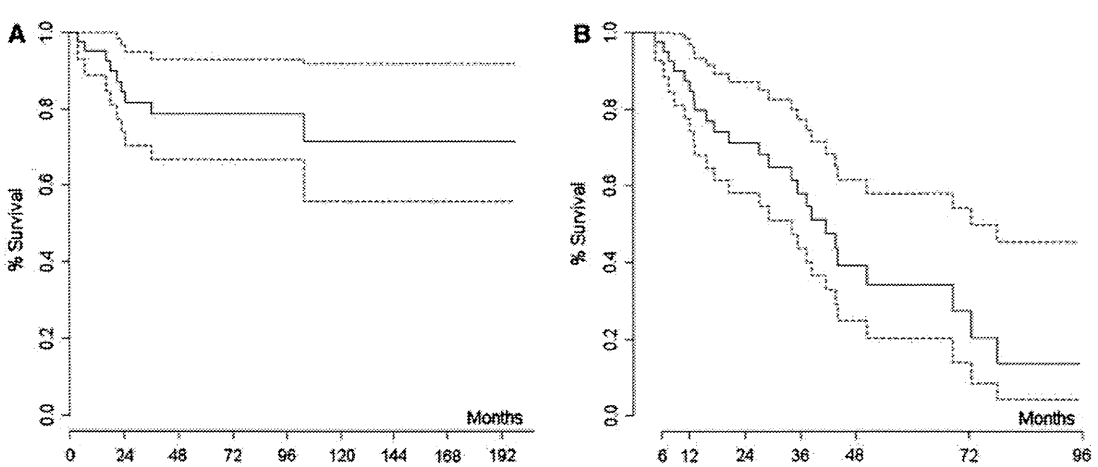

Fig. 2 Kaplan–Meier estimation of overall survival and the 95 % confidence intervals (**a**) and of relapse-free survival and the 95 % confidence intervals (**b**)

Table 3 Univariate analysis of overall and progression-free survival for the qualitative data

	Overall survival		Progression-free survival	
	Events/Patients (%)[a]	*p* value	Events/Patients (%)[a]	*p* value
Sex		0.57		0.89
Male	5/21 (23.8 %)		10/21 (47,6 %)	
Female	4/23 (17,4 %)		14/23 (60.9 %)	
Type of surgery		0.04		0.18
Biopsy	3/6 (50.0 %)		3/6 (50.0 %)	
Gross total resection	3/26 (11.5 %)		13/26 (50.0 %)	
Partial resection	3/12 (25.0 %)		9/12 (75.0 %)	
Chemotherapy		0.49		0.86
Yes	1/8 (12.5 %)		5/8 (62.5 %)	
No	8/36 (22.2 %)		20/36 (55.5 %)	
Radiotherapy		0.12		0.15
Yes	8/28 (28.6 %)		15/28 (53.6 %)	
No	1/16 (6.2 %)		10/16 (62.5 %)	

[a] Percentage of events (death or relapse), *p* values in the Log-Rank test <0.05 were considered significant

heterogeneously enhancing masses, and are usually associated with obstructive hydrocephalus [10, 11, 14, 20, 21]. They are difficult to distinguish from other clinical entities, especially pineocytomas [10, 14]. T2-weighted MRI often reveals heterogeneous, hyperintense regions, whereas T1-weighted imaging often reveals low-to-intermediate intensities [11, 13, 22]. However, hyperintensity on non-contrast T1-weighted sequences has been described in some patients presenting with PTPR, which might be explained by high concentrations of proteins in the small cystic spaces seen in these neoplasms [23–28]. However, this hyperintensity was not found in other cases [11, 25], suggesting a variation in radiographic findings in different lesions. In two reported cases, proton MR spectroscopy revealed increased choline and decreased N-acetyl aspartate peaks and a slightly increased lactate peak [13, 26]. Positron emission tomography has shown increased 18-fluorodeoxyglucose uptake at the site of the lesion, suggesting a malignant tumor with increased glucose metabolism [13]. Further studies are required to validate these results obtained in case reports of PTPR.

Data on treatment options and their outcomes have only been published for small series, and prognostic factors and formal consensus guidelines for optimal management of patients presenting with PTPR are not yet well established. Our study showed that the extent of surgery was identified on univariate analysis as the only clinical factor significantly associated with a better OS, highlighting the importance of surgery as the primary mainstay of therapy for PTPR. This result confirms the tendency for gross total resection to be associated with better OS and PFS previously reported with fewer patients [4]. As PTPRs may be derived from subcommissural modified ependymocytes, the clinical behavior of PTPRs can be compared to that of ependymomas. The effect of the extent of tumor removal has been well documented in intracranial ependymomas in adults by some authors [29–34], more particularly when the extent of resection was adequately evaluated. The initial treatment of choice for PTPRs, as in ependymomas, seems to be complete resection whenever safely feasible.

The role of radiotherapy in the treatment of patients presenting with PTPR is not established. Our results showed that radiotherapy did not influence OS or PFS, but the number of patients treated was quite low. This negative result may be due to the retrospective nature of our study, which involved heterogeneous radiotherapy regimens in the different centers. As the prognosis for PTPRs seems to be similar to that of ependymomas, with a propensity for local recurrence, many institutions treat the patient with post operative radiotherapy. The precise role of radiotherapy in ependymomas, more particularly the optimal dose, timing, and field size, is still debated, but its seems that adjuvant radiotherapy may be beneficial to control disease locally [34, 35]. Adjuvant radiotherapy was frequently used in the PTPR cases reported [8, 9, 13, 14, 20–22, 24, 27, 36–43]. Prospective studies are required to analyze the role of radiotherapy in PTPRs, more particularly after incomplete resection or when surgery cannot be performed.

The role of chemotherapy in the treatment of patients presenting with PTPR is also poorly documented. Only a few cases of PTPRs treated with chemotherapy have been reported previously [4, 11, 16, 44]. Our results showed that chemotherapy did not influence OS or PFS. One patient with a PTPR that recurred after surgery and radiotherapy was treated with temozolomide and is still symptom-free 9 years after the first treatment [44]. This alkylating drug can inhibit all stages of tumor cell growth and may present some advantages in patients with PTPRs. Although hypermethylation of the

promotor of the O6-methylguanine-DNA-methyltransferase gene has not been described in PTPRs, in other brain tumors, such as glioblastoma, it has been shown to be associated with improved outcome and may be a predictive marker of sensitivity to alkylating agents [45].

Our series further confirms the high rate of recurrence in PTPR, which accounted for 58 % at 5 years and greater than 70 % at 6 years. This high rate of recurrence is similar to that reported for intracranial ependymomas [46]. Recurrences were more often local and 13 patients underwent only one relapse (local or not). Spinal dissemination seems to be rare and was only seen in 3 cases. Some cases of PTPR may be more aggressive and have a potential for seeding into the spinal canal, particularly if complete tumor resection cannot be achieved [4, 47].

In conclusion, these data confirm the high risk of recurrence in PTPR and emphasize the importance of gross total resection, while adjuvant radiotherapy or chemotherapy failed to exert significant effects on OS and PFS.

Acknowledgments We thank the pathologists H. Adle Biassette (Créteil), C. Bouvier (Marseille), F. Chrétien (Créteil), C. Christov (Créteil), N. Costes-Charlet (Clermont-Ferrand), C. Daumas-Duport (Paris), M.B. Delisle (Toulouse), C. Fernandez (Marseille), R. Gherardi (Créteil), J.M. Goujon (Poitiers), B. Grignon (Nancy), A. Heitzmann (Orléans), D. Henin (Paris), J.L. Kemeny (Clermont-Ferrand), N. Kopp (Lyon), K. Kuchelmeister (Giessen), M. Kujas (Paris), A. Lellouch-Tubiana (Paris), J.F. Michiels (Nice), J. Mikol (Paris), N. Streichenberger (Lyon), M. Yver (Poitiers); the neurosurgeons B. Bataille (Poitiers), H. Boissonnet (Paris), P. Bousquet (Toulouse), P. Bret (Lyon), S. Clemenceau (Paris), P. Decq (Créteil), H. Dufour (Marseille), G. Fisher (Lyon), S. Fuentes (Marseille), T. Inoue (Sendai), B. Irthum (Clermont-Ferrand), P. Kauffmann (Clermont-Ferrand), M. Kalamarides (Paris), A. Morita (Tokyo), B. Muckensturm (Orléans), I. Pelissou-Guyotat (Lyon), J. Remond (Lyon), C. Sainte-Rose (Paris), M. Samii (Hannover), and M. Sindou (Lyon); the neuro-oncologists L. Taillandier (Nancy), M. Frenay (Nice), O. Chinot (Marseille), J. Honnorat (Lyon), B. Wrede (Regensburg), and J.E. Wolff (Regensburg); the radiotherapists M. Benhassel (Rennes), R.J. Bensadoun (Poitiers), P.Y. Bondiau (Nice), S. Hoffstetter (Nancy), J.J. Mazeron (Paris), F. Mornex (Lyon), and M. Schlienger (Paris); E. Chamorey (Nice) for statistical anlysis and T. Barkas for linguistic help.This work was supported by the association ADeRTU and INSERM.

Ethical standards The present experiments comply with the current laws of the countries in which they were performed.

Conflict of interest The authors declare that they have no conflict of interest.

References

1. Nakazato Y, Jouvet A, Scheithauer BW (2007) Tumours of the pineal region. In: Louis DN, Ohgaki H, Wiestler OD, Cavenee WK (eds) WHO classification of tumours of the central nervous system. International Agency for Research on Cancer, Lyon, pp 122–127
2. Jouvet A, Fauchon F, Liberski P, Saint-Pierre G, Didier-Bazes M, Heitzmann A, Delisle MB, Adle-Biassette A, Vincent S, Mikol J, Streichenberger N, Ahboucha S, Brisson C, Belin MF, Fèvre Montange M (2003) Papillary tumor of the pineal region. Am J Surg Pathol 27:505–512
3. Jouvet A, Nakazato Y, Scheithauer BW, Paulus W (2007) Papillary tumour of the pineal region. In: Louis DN, Ohgaki H, Wiestler OD, Cavenee WK (eds) WHO classification of tumours of the central nervous system. International Agency for Research on Cancer, Lyon, pp 128–129
4. Fèvre Montange M, Hasselblatt M, Figarella-Branger D, Chauveinc L, Champier J, Saint-Pierre G, Taillandier L, Coulon A, Paulus W, Fauchon F, Jouvet A (2006) Prognosis and histopathologic features in papillary tumors of the pineal region: a retrospective multicenter study of 31 cases. J Neuropathol Exp Neurol 65:1004–1011
5. Hasselblatt M, Blümcke I, Jeibmann A, Rickert CH, Jouvet A, van de Nes JA, Kuchelmeister K, Brunn A, Fèvre Montange M, Paulus W (2006) Immunohistochemical profile and chromosomal imbalances in papillary tumours of the pineal region. Neuropathol Appl Neurobiol 32:278–283
6. Buffenoir K, Rigoard P, Wager M, Ferrand S, Coulon A, Blanc JL, Bataille B, Listrat A (2008) Papillary tumor of the pineal region in a child: case report and review of the literature. Childs Nerv Syst 24:379–384
7. Jeruc J, Popovic M (2008) Papillary tumor of the pineal region, a case report. Clin Neuropathol 27:192
8. Lechapt-Zalcman E, Chapon F, Guillamo JS, Khouri S, Menegalli-Boggelli D, Loussouarn D, Fèvre Montange M, Jouvet A (2011) Long-term clinicopathological observations on a papillary tumour of the pineal region. Neuropathol Appl Neurobiol 37:431–435. doi:10.1111/j.1365-2990.2010.01133.x
9. Santarius T, Joseph JA, Tsang KT, O'Donovan DG, Kirollos RW (2008) Papillary tumour of the pineal region. Br J Neurosurg 22:116–120
10. Amemiya S, Shibahara J, Aoki S, Takao H, Ohtomo K (2008) Recently established entities of central nervous system tumors: review of radiological findings. J Comput Assist Tomogr 32: 279–285
11. Shibahara J, Todo T, Morita A, Mori H, Aoki S, Fukayama M (2004) Papillary neuroepithelial tumor of the pineal region. A case report. Acta Neuropathol 108:337–340
12. Fèvre Montange M, Grand S, Champier J, Hoffmann D, Pasquier B, Jouvet A (2008) Bcl-2 expression in a papillary tumor of the pineal region. Neuropathology 28:660–663
13. Inoue T, Kumabe T, Kanamori M, Sonoda Y, Watanabe M, Tominaga T (2008) Papillary tumor of the pineal region: a case report. Brain Tumor Pathol 25:85–90
14. Poulgrain K, Gurgo R, Winter C, Ong B, Lau Q (2011) Papillary tumour of the pineal region. J Clin Neurosci 18:1007–1017
15. Rickard KA, Parker JR, Vitaz TW, Plaga AR, Wagner S, Parker JC (2011) Papillary tumor of the pineal region: two case studies and a review of the literature. Ann Clin Lab Sci 41:174–181
16. Santoro A, D'Elia A, Fazzolari B, Santoro F, Antonelli M, Giangaspero F, Brogna C, Lenzi J, Frati A, Salvatti M (2012) Four-year clinical and neuroradiological follow-up of a papillary tumor of the pineal region. Neurol Sci 33:931–935. doi: 10.1007/s10072-011-0860-5
17. Marcol W, Kotulska K, Grajkowska W, Gołka D, Własczuk P, Drogosiewicz M, Mandera M, Lewin-Kowalik J, Roszkowski M (2007) Papillary pineocytoma in child: A case report. Biomed Pap med Fac Univ Palacky Olomouc Czech Repub 151: 121–123
18. Li J, Recinos PF, Orr BA, Burger PC, Jallo GI, Recinos VR (2011) Papillary tumor of the pineal region in a 15-month-old boy. J Neurosurg Pediatr 7:534–538

19. Abela L, Rushing EJ, Ares C, Scheer I, Bozinov O, Boltshauser E, Grotzer MA (2012) Pediatric papillary tumors of the pineal region: to observe or to treat following gross total resection? Childs Nerv Syst. doi:10.1007/s00381-012-1935-1
20. Kern M, Robbins P, Lee G, Watson P (2006) Papillary tumor of the pineal region-a new pathological entity. Clin Neuropathol 25:185–192
21. Junior GV, Dellaretti M, de Carvalho GT, Brandao RACS, Mafra A, de Sousa AA (2011) Papillary tumor of the pineal region. Brain Tumor Pathol 28:329–334
22. Sharma MC, Jain D, Sarkar C, Suri V, Garg A, Sharma BS, Mehta VS (2009) Papillary tumor of the pineal region, a recently described entity: a report of three cases and review of the literature. Clin Neuropatol 28:295–302
23. Chang AH, Fuller GN, Debnam JM, Karis JP, Coons SW, Ross JS, Dean BL (2008) MR imaging of papillary tumor of the pineal region. AJNR Am J Neuroradiol 29:187–189
24. Cerase A, Vallone IM, Di Pietro G, Oliveri G, Miracco C, Venturi C (2009) Neuroradiological follow-up of the growth of papillary tumor of the pineal region: a case report. J Neurooncol 95:433–435
25. Sato TS, Kirby PA, Buatti JM, Moritani T (2009) Papillary tumor of the pineal region: report of a progressive tumor with possible multicentric origin. Pediatr Radiol 39:188–190
26. Vaghela V, Radhakrishnan N, Radhakrishnan VV, Menon G, Kesavadas C, Thomas B (2010) Advanced magnetic resonance imaging with histopathological correlation in papillary tumor of pineal region: report of a case and review of literature. Neurol India 58:928–932
27. Patel SK, Tomei KL, Christiano LD, Baisre A, Liu JK (2012) Complete regression of papillary tumor of the pineal region after radiation therapy: case report and review of the literature. J Neurooncol 107:427–434
28. Vandergriff C, Opatowsky M, O'Rourke B, Layton K (2012) Papillary tumor of the pineal region. Proc (Bayl Univ Med Cent) 25:78–79
29. Kawabata Y, Takahashi JA, Arakawa Y, Hashimoto N (2005) Long-term outcome in patients harboring intracranial ependymoma. J Neurooncol 103:31–37
30. Metellus P, Barrie M, Figarella-Branger D, Chinot O, Giorgi R, Gouvernet J, Jouvet A, Guyotat J (2007) Multicentric French study on adult intracranial ependymomas: prognostic factors analysis and therapeutic consideration from a cohort of 152 patients. Brain 130:1338–1349
31. Metellus P, Figarella-Branger D, Guyotat J, Barrie M, Giorgi R, Jouvet A, Chinot (2008) Supratentorial ependymomas: prognostic factors and outcome analysis in a retrospective series of 46 adult patients. Cancer 113:175–185
32. Guyotat J, Metellus P, Giorgi R, Barrie M, Jouvet A, Fèvre Montange M, Chinot O, Durand A, Figarella-Branger D (2009) Infratentorial ependymomas: prognostic factors and outcome analysis in a multi-center retrospective series of 106 adult patients. Acta Neurochir 151:947–960
33. Boström A, Boström J, Hartmann W, Pietsch T, Feuss M, von Lehe M, Simon M (2011) Treatment results in patients with intracranial ependymomas. Cen Eur Neurosurg 72:127–132. doi: 10.1055/s-0031-1273745
34. Swanson EL, Amdur RJ, Morris CG, Galloway TJ, Marcus RB Jr, Pincus DW, Smith A (2011) Intracranial ependymomas treated with radiotherapy: long-term results from a single institution. J Neurooncol 102:451–457
35. Pejavar S, Polley MY, Rosenberg-Wohl S, Chennupati S, Prados MD, Berger MS, Banerjee A, Gupta N, Haas-Kogan D (2012) Pediatric intracranial ependymoma: the roles of surgery, radiation and chemotherapy. J Neurooncol 106:367–375
36. Dagnew E, Langford LA, Lang FF, DeMonte F (2007) Papillary tumors of the pineal region: case report. Neurosurgery 60: E953–E955
37. Boco T, Aalaei S, Musacchio M, Byrne R, Cochran E (2008) Papillary tumor of the pineal region. Neuropathology 28:87–92
38. Nakamura H, Makino K, Kochi M, Nakazato Y, Kuratsu J (2009) Successful treatment of neoadjuvant therapy for papillary tumor of the pineal region. Brain Tumor Pathol 26:73–77
39. Yano H, Ohe N, Nakayama N, Shinoda J, Iwama T (2009) Clinicopatological features from long-term observation of a papillary tumor of the pineal region (PTPR): a case report. Brain Tumor Pathol 26:83–88
40. Kim YH, Kim JW, Park CK, Kim DG, Sohn CH, Chang KH, Park SH (2010) Papillary tumor of pineal region presenting with leptomeningeal seeding. Neuropathology 30:654–660. doi: 10.1111/j.1440-1789.2010.01108.x
41. Epari S, Bashyal R, Malick S, Gupta T, Moyadi A, Kane SV, Bal M, Jalali R (2011) Papillary tumor of pineal region: report of three cases and review of literature. Neurol India 59:455–460
42. Matyja E, Grakowska W, Nauman P, Bonicki W (2011) Histopathological patterns of papillary tumour of the pineal region. Folia Neuropathol 49:181–190
43. El Majdoub F, Blau T, Hoevels M, Buhrle C, Deckert M, Treuer H, Sturm V, Maarouf M (2012) Papillary tumors of the pineal region: a novel therapeutic option-streotactic 125iodine brachytherapy. J Neurooncol 109:99–104. doi:10.1007/s11060-012-0870-z
44. Lorenzetti M, Motta F, Campanella R, Bauer D, Assi A, Arienta C, Gaini SM, Caroli M (2011) Adjuvant temozolomide chemotherapy for treatment of papillary tumor of the pineal region. World Neurosurg 76:160–163
45. Rivera AL, Pelloski CE, Gilbert MR, Colman H, De La Cruz C, Sulman EP, Bekele BN, Aldape KD (2010) MGMT promoter methylation is predictive of response to radiotherapy and prognostic in the absence of adjuvant alkylating chemotherapy for glioblastoma. Neurooncol 12:116–121
46. Ernestus RI, Schroder R, Stutzer H, Klug N (1997) The clinical and prognostic relevance of grading in intracranial ependymomas. Br J Neurosurg 11:421–428
47. Hong B, Nakamura M, Brandis A, Becker H, Krauss JK (2011) Spinal metastasis of papillary tumor of the pineal region. Clin Neurol Neurosurg 113:235–238

DOI: 10.3171/2013.1.PEDS11449

Dynamic changes in magnetic resonance imaging appearance of dysembryoplastic neuroepithelial tumor with or without malignant transformation

Report of 2 cases

Yui Mano, M.D.,[1] Toshihiro Kumabe, M.D., Ph.D.,[1] Ichiyo Shibahara, M.D.,[1] Ryuta Saito, M.D., Ph.D.,[1] Yukihiko Sonoda, M.D., Ph.D.,[1] Mika Watanabe, M.D., Ph.D.,[2] and Teiji Tominaga, M.D., Ph.D.[1]

[1]*Department of Neurosurgery, Tohoku University Graduate School of Medicine; and* [2]*Department of Pathology, Tohoku University Hospital, Sendai, Miyagi, Japan*

Dysembryoplastic neuroepithelial tumors (DNETs) have conventionally been regarded as benign and stable tumors and considered curable with surgery without adjunctive therapy. Recently, recurrent DNETs with or without malignant transformation have been described. The authors report 2 unusual cases of DNET: 1) an enlarging lesion that developed an enhancing component over the natural course of 4 years, and 2) a recurrent DNET that developed an enhancing component 10–11 years after gross-total resection. The patient in the first case was treated with subtotal resection and adjuvant radiochemotherapy; histological examination of the tumor led to the diagnosis of DNET, WHO Grade I, for the nonenhancing component and anaplastic oligodendroglioma, WHO Grade III, for the enhancing component. The patient in the second case was treated with repeat gross-total resection; the original tumor had been histologically diagnosed as DNET, and the nonenhancing and enhancing components of the recurrent tumor were diagnosed as simple and complex forms of DNET, respectively. These and previous reports suggest an aggressive subtype of DNETs. If follow-up MRI reveals progressive behavior, resection should be performed without delay. Additional radiochemotherapy is needed if the histological diagnosis demonstrates malignant transformation.
(http://thejns.org/doi/abs/10.3171/2013.1.PEDS11449)

Key Words • **dysembryoplastic neuroepithelial tumor** • **oncology** • **magnetic resonance imaging** • **malignant transformation** • **recurrence**

Dysembryoplastic neuroepithelial tumor is a benign, usually supratentorial glial-neuronal neoplasm classified as a WHO Grade I tumor and characterized by a predominantly cortical location and by drug-resistant partial seizures. These lesions typically have a complex columnar and multinodular architecture and are often associated with cortical dysplasia.[3] DNET tends to occur in children or young adults and was first described by Daumas-Duport and colleagues.[3,4] The tumor appears hypodense on CT, hypointense on T1-weighted MRI, and hyperintense on T2-weighted MRI,[6] with enhancement on T1-weighted MR images obtained after Gd administration in 18%–33% of cases.[4,15,16] DNETs may exhibit changes in the MRI pattern over time; the development of enhancement does not necessarily imply malignant transformation,[10] but true malignant transformation of DNETs has been reported recently.[8,11,12]

We describe 2 cases of DNET demonstrating dynamic radiographic changes during their clinical courses, with or without malignant transformation. We analyzed *IDH1/2* mutation by direct sequencing with immunohistochemistry and copy number changes for 1p, 7p *(EGFR)*, 9p *(CDKN2A)*, 10q *(PTEN)*, chromosome 17 (*TP53* and *ERBB2*), and 19q by multiple ligation-dependent probe amplification. This retrospective study was conducted under approval of the ethics committee of Tohoku University School of Medicine, and written informed consent was obtained from the parents of both patients.

This article contains some figures that are displayed in color online but in black-and-white in the print edition.

Abbreviations used in this paper: CDKN2A = cyclin-dependent kinase inhibitor 2A; DNET = dysembryoplastic neuroepithelial tumor; *EGFR = epidermal growth factor receptor*; *ERBB2 = v-erb-b2 erythroblastic leukemia viral oncogene homolog 2*; GFAP = glial fibrillary acidic protein; *IDH1/2 = isocitrate dehydrogenase 1 and 2*; NFP = neurofilament protein; Olig2 = oligodendrocyte transcription factor 2; *PTEN = phosphatase and tensin homolog*; SYN = synaptophysin; *TP53 = tumor protein p53*; WHO = World Health Organization.

Case Reports

Case 1

History and Presentation. This 4-year-old girl was referred to our department with enlargement of a lesion in the right parietal region appearing as low density on CT after a follow-up period of 4 years.

She had suffered a complex partial seizure localized in the left upper limb 10 months after birth. She was taken to a hospital with a pediatric department, and neuroimaging was performed. Head CT revealed a right parietal low-density lesion (Fig. 1A). T1-weighted MRI with Gd administration did not demonstrate any enhancing lesion at this point (Fig. 1B), but FLAIR imaging did show a hyperintense lesion predominantly in the right primary sensory area, corresponding to the low-density lesion on CT (Fig. 1C). Her seizures were controlled by antiepileptic drug therapy. Follow-up CT was performed at age 4 years. The right parietal low-density area had enlarged and a high-density spot within this area was suspicious for calcification (Fig. 1D). She was then referred to our department.

Examination. On admission, the child had no neurological deficit. T1-weighted MRI demonstrated a hyperintense ring corresponding to the area of possible calcification within the large hypointense lesion, with ring enhancement within this hyperintense ring by Gd administration (Fig. 1E). T2-weighted MRI showed a hyperintense lesion that corresponded with the hypointense lesion on T1-weighted images (Fig. 1F).

Operation and Postoperative Course. The patient underwent subtotal resection including total resection of the area of enhancement (Fig. 1G), but not the precentral gyrus and pyramidal tract with tumor invasion. Intraoperatively, tissue samples were obtained from both the enhancing lesion confirmed by a neuronavigation system and the surrounding nonenhancing lesion.

Pathological Examination. Histological examination of the area that appeared hypointense on T1-weighted MRI showed multiple cystic structures with myxomatous background and proliferation of oligodendroglia-like cells with oval nuclei in the wall of the cystic spaces (Fig. 2A). Neuronal elements with "floating neurons" were found, indicating a glioneuronal lesion, within the cystic cavity (Fig. 2B arrows). Immunohistochemical analysis revealed intensely positive staining for Olig2 (Immuno-Biological Laboratories; 1:500) and less reactivity for GFAP (DAKO; clone 6F2, 1:100) in the glial component, and positive reaction for NFP (DAKO; clone 2F11, 1:100) and SYN (DAKO; clone SY38, 1:300) in the neuronal elements (Fig. 2C–E, SYN not shown). The Ki 67 (DAKO; clone MIB-1, 1:30) labeling index was 2% (Fig. 2F). Therefore, the main part of the tumor, appearing as hypointense on T1-weighted MR images, was diagnosed as DNET, WHO Grade I.

Histological examination of tissue from the enhancing

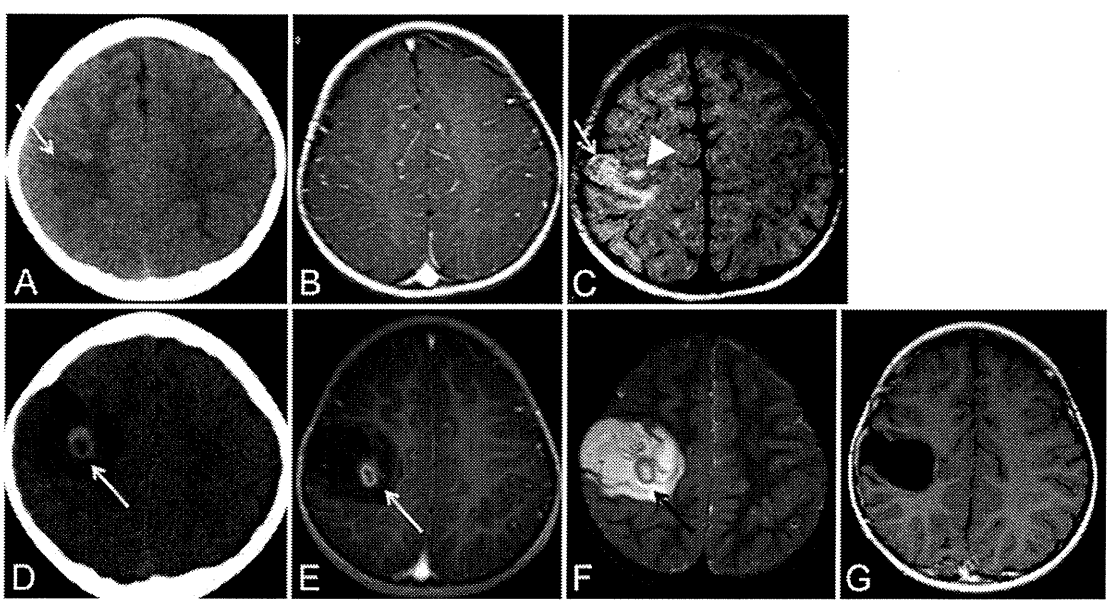

Fig. 1. Case 1. Axial CT and MR images obtained 10 months after birth **(A–C)** and at age 4 years **(D–F)** and postoperative follow-up MR image **(G)**. **A:** CT scan showing a slightly hypodense lesion in the right hemisphere *(arrow)*. **B:** T1-weighted MR image obtained after Gd administration demonstrating no enhancement. **C:** FLAIR MR image disclosing a hyperintense lesion predominantly in the right postcentral gyrus *(arrow)*, with invasion into the right precentral knob *(arrowhead)*. **D:** CT scan clarifying marked enlargement of the hypodense lesion, with an emerging hyperdense ringlike nodule inside the lesion *(arrow)*. **E:** T1-weighted MR image obtained after Gd administration showing ringlike enhancement *(arrow)* inside the hyperintense rim on the T1-weighted MR image obtained without Gd (not shown). **F:** T2-weighted MR image depicting a hyperintense lesion predominantly in the right postcentral gyrus corresponding to the hypointense lesion on the T1-weighted MR image. The hyperintense rim on the T1-weighted MR image appears as hypointense on the T2-weighted MR image *(arrow)*. **G:** Postoperative axial T1-weighted MR image obtained after Gd administration demonstrating no enhancing lesion.

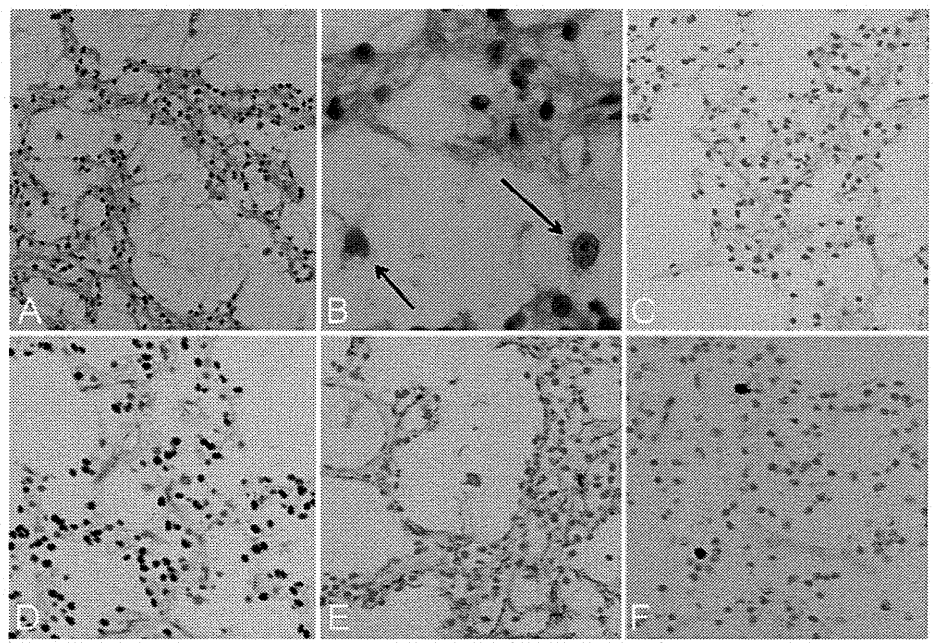

Fig. 2. Case 1. Photomicrographs of the surgical specimen from the lesion that showed no Gd enhancement on MRI. **A:** Multiple cystic structures are observed on a mucinous background. H & E, original magnification ×100. **B:** High-power view of A, showing floating neurons *(arrows)* scattered in the cystic structure. H & E, original magnification ×400. **C–E:** Immunostaining for GFAP (C), Olig2 (D), and NFP (E) are all positive. Original magnification ×100. **F:** The Ki 67 labeling index was 2%. Original magnification ×100.

component demonstrated atypical glial cells with swollen oval nuclei, proliferating with a high cellular density (Fig. 3A). A meshwork of capillary-like vasculature showing a chicken-wire appearance had developed among the glial cells, and focal microvascular proliferation (that is, piling up of the endothelial cells with glomeruloid appearance) was observed (Fig. 3B). Immunochemical analysis showed markedly positive staining for Olig2, only focal

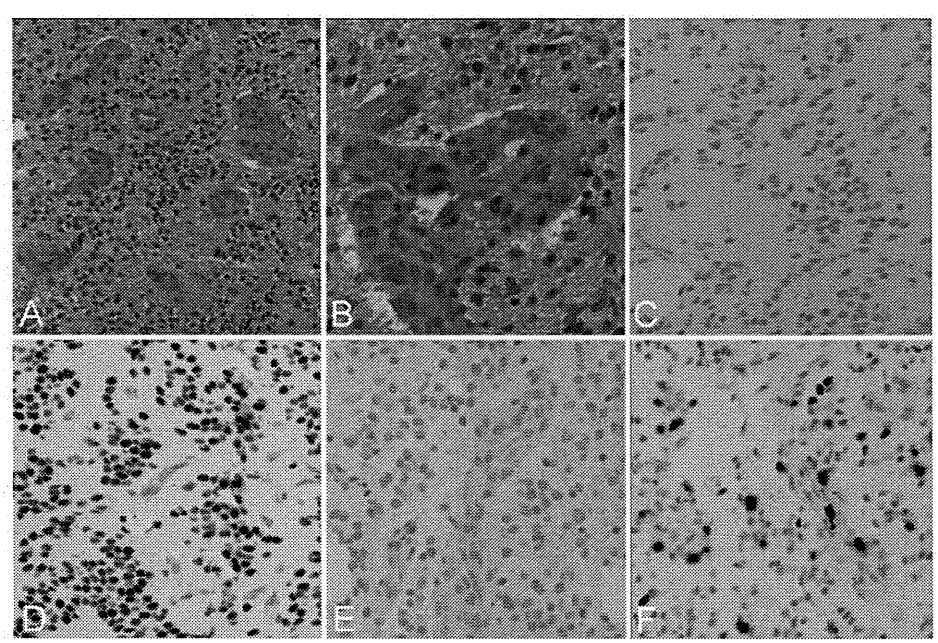

Fig. 3. Case 1. Photomicrographs of the surgical specimen from the lesion that showed enhancement on MRI. **A:** Markedly proliferated atypical glial cells and chicken-wire appearances are observed. H & E, original magnification ×100. **B:** High-power view of A, showing microvascular proliferation. H & E stain, original magnification ×400. **C–E:** Immunostaining for GFAP (C) and NFP (E) are negative, but Olig2 (D) is strongly positive. Original magnification ×100. **F:** The Ki 67 labeling index was focally up to 30%. Original magnification ×100.

positive staining for GFAP, and no positive staining for NFP or SYN (Fig. 3C–E, SYN not shown). The Ki 67 labeling index was focally up to 30% (Fig. 3F).

Immunochemical staining for IDH1 R132H (Dianova; clone H09, 1:400) was negative in both nonenhancing and enhancing components of the lesion (data not shown). The diagnosis of the enhancing component was anaplastic oligodendroglioma, WHO Grade III. The molecular profile of the nonenhancing component was wild-type *IDH1/2* and no chromosomal copy changes of *TP53*, *PTEN*, *EGFR*, *CDKN2A*, *ERBB2*, and 1p/19q (Table 1). No molecular profile of the enhancing component was obtained.

Additional Treatment and Postoperative Course. Adjuvant therapy consisted of 60-Gy fractionated radiation to the extended local field. Nimustine hydrochloride (ACNU) was administered intravenously at 100 mg/m^2 body surface area on the first day of radiation therapy. The child was discharged home 7 weeks after the surgery without neurological deficit. She was treated with maintenance ACNU therapy bimonthly (6 times per year) at an outpatient clinic, and follow-up MR images obtained 20 months after surgery disclosed no tumor recurrence.

Case 2

Initial Presentation and Imaging. This 3-year-old boy was initially referred to our hospital with simple partial seizures localized to the left side of the face. On admission, neuroimaging showed a tumor located in the right facial motor cortex (Fig. 4A).

First Operation and Postoperative Course. A craniotomy and gross-total resection were performed (Fig. 4B). The histological diagnosis was DNET. The boy was discharged home, treated with antiepileptic drug therapy, and followed up with regular MRI.

At age 14, he began to experience partial seizures again, this time localized to the left upper limb. At that time he was a student in regular junior high school. Gadolinium-enhanced T1-weighted MRI revealed an enhancing lesion located on the upper posterior aspect of the previous resection cavity (Fig. 4C); the lesion had not been evident 1 year previously. Tumor recurrence was suspected, and the patient was admitted to our hospital for surgery.

Second Operation. On this second admission, the boy was neurologically intact. Gross-total resection of the tumor was performed with motor evoked potential monitoring. Intraoperatively, the enhancing component (as confirmed by an intraoperative neuronavigation system) was not macroscopically differentiated from the surrounding nonenhancing component lesion.

Pathological Examination. Histological examination of the nonenhancing component demonstrated glioneuronal elements in a columnar orientation on a mucinous background. Similar to Case 1, proliferation of oligodendroglia-like cells with oval nuclei was observed in the wall of the cystic spaces (Fig. 5A). The cystic cavities contained "floating neurons" surrounded by oligodendroglioa-like glial cells (Fig. 5B). Immunochemical staining showed a positive reaction for GFAP and Olig2 in the glial component and a positive reaction for NFP and SYN in the neuronal element (Fig. 5C–E, SYN not shown). The Ki 67 labeling index was 2% (Fig. 5F).

Histological examination of the enhancing component demonstrated an oligodendroglioma-like appearance with proliferation of small vessels with increased endothelial

TABLE 1: Immunohistochemistry and genetic profiles of the enhancing and nonenhancing lesion components*

Parameter	Case 1		Case 2	
	Nonenhancing	Enhancing	Nonenhancing	Enhancing
histological diagnosis	DNET (S)	AO	DNET (S)	DNET (C)
immunostaining				
GFAP	+	–	+	+
Olig2	+	+	+	+
NFP	+	–	+	–
SYN	+	–	+	–
IDH1	–	–	–	–
Ki 67 labeling index (%)	2	30	2	2
genetic profile				
IDH1/2	wild/wild	NA	wild/wild	NA
TP53†	retain	NA	retain	NA
PTEN†	retain	NA	retain	NA
EGFR†	retain	NA	retain	NA
CDKN2A†	retain	NA	retain	NA
ERBB2†	retain	NA	retain	NA
1p & 19q†	retain	NA	retain	NA

* AO = anaplastic oligodendroglioma; DNET (C) = DNET, complex form; DNET (S) = DNET, simple form; NA = not available.
† Analyzed chromosome copy number change.

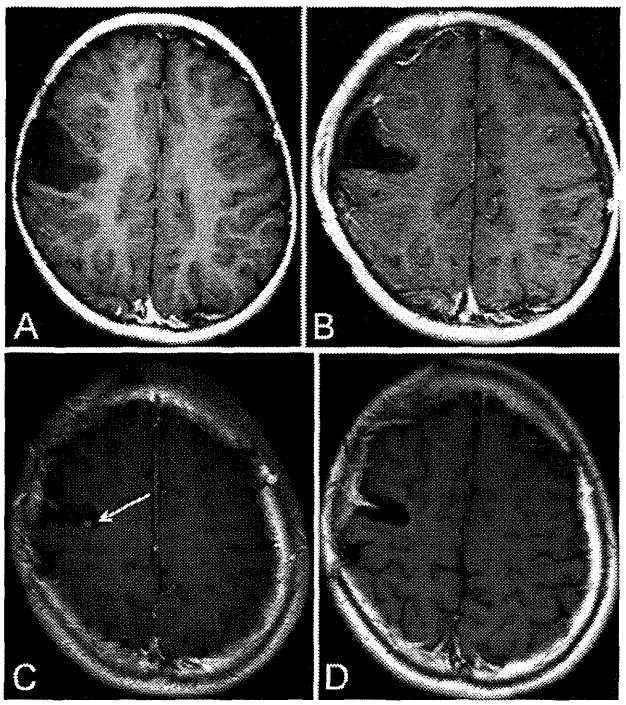

FIG. 4. Case 2. Axial T1-weighted MR images obtained after Gd administration before (A) and after (B) the first operation (at age 3 years) and before (C) and after (D) the second operation (at age 14 years). A: Preoperative image showing a hypointense nonenhancing lesion in the right facial motor area. B: Postoperative image showing total resection. C: Imaging performed 11 years later revealed a hypointense lesion with an enhancing area (*arrow*) that was not evident on earlier studies. D: Postoperative image showing no enhancing lesion.

prominence (Fig. 6A and B). However, the typical piled-up, multilayered appearance of endothelial cells in the typical microvascular proliferation was absent. Immunochemical staining showed a positive reaction for GFAP and Olig2 (Fig. 6C and D), but was negative for NFP and SYN (Fig. 6E, SYN not shown). The Ki 67 labeling index was 2% (Fig. 6F).

Immunochemical staining for IDH1 R132H was negative in both the nonenhancing and enhancing components (data not shown); the histological diagnoses were simple and complex forms of DNET, respectively. The molecular profiles of the nonenhancing component of the tumor were wild-type *IDH1/2*, and no copy changes of *TP53*, *PTEN*, *EGFR*, *CDKN2A*, *ERBB2*, and 1p/19q (Table 1). No molecular profiles of the enhancing component were obtained.

Based on the histological diagnosis and gross-total resection, no additional radiochemotherapy was performed, and the patient was discharged home without neurological deficit. He was followed up with regular MRI, and at the most recent MRI examination, 33 months after the second surgery, no tumor recurrence was detected (Fig. 4D).

Discussion

Is DNET a Benign, Stable Lesion?

Dysembryoplastic neuroepithelial tumor has always been regarded as a benign quasi-hamartomatous lesion. It has been divided into 3 subtypes: the simple form, complex form, and nonspecific form.[3–5] The simple form contains only the "specific glioneuronal element" consisting of intracortical oligodendrocyte-like cells and floating neurons, in which ganglion cells appear to be "floating" within pools of basophilic mucinous matrix. The complex form also includes glial nodules, which are most often patterned and mucin-rich, containing mostly oligodendrocyte-like cells.[3,4] The nonspecific form remains highly controversial since it contains neither of these pathological hallmarks; instead it resembles a diffuse glioma but is confined to the cortex.[5] Unfavorable histological findings such as nuclear atypia, mitosis, microvascular proliferation, or high cell density have not suggested malignant gliomas and had no prognostic significance in DNETs. The Ki 67 labeling index should not be used to distinguish DNETs from ordinary gliomas unless the lesion is stable.[5] Actually, most DNETs show very low proliferative activity, with Ki 67 labeling indices usually lower than 1%. However, elevated Ki 67 labeling indices have been reported in some cases, especially the complex and nonspecific forms.[13,14] Our present cases and other recent reports suggest that DNETs may have the potential to undergo dramatic changes such as malignant transformation. All cases with malignant transformation had high Ki 67 labeling index values (Table 2), and the tumors demonstrated aggressive behavior.[8,11,12] Therefore, neurosurgeons must recognize that DNETs have progressive potential.

Histological Correlations With Neuroimaging Findings

Generally, DNET appears as a low-density area on CT, a well-demarcated low-intensity area on T1-weighted MRI, and a high-intensity area on T2-weighted MRI, with nodular, ringlike, or heterogeneous contrast enhancement in 20% of cases. Calcifications are generally observed in approximately 40% of DNETs. The MRI findings correspond to the histological findings as follows: the glioneuronal element, characterized by oligodendrocyte-like cells and floating neurons, has the conventional neuroimaging appearance, whereas the enhancing regions occasionally contain glomeruloid vessels, usually in the vicinity of enhancing tumor classified as the complex type.[1,16] Additionally, DNETs may exhibit a changing MRI pattern over time, and the development of enhancement does not necessarily imply malignant transformation.[10] Enhancement on MR images was observed in our 2 cases, diagnosed as anaplastic oligodendroglioma and as the complex form of DNET. Clearly, enhancement on neuroimaging does not always correspond to malignant transformation.[1,10,16] However, 3 cases of malignant transformation of DNET have been reported with enhancement on MRI (Table 2).[8,11,12] Therefore, malignant transformation should be considered if enhancement occurs.

Comparison With Previous Cases of Malignant Transformation

Several cases of malignant transformation of DNET have been reported (Table 2).[8,11,12]

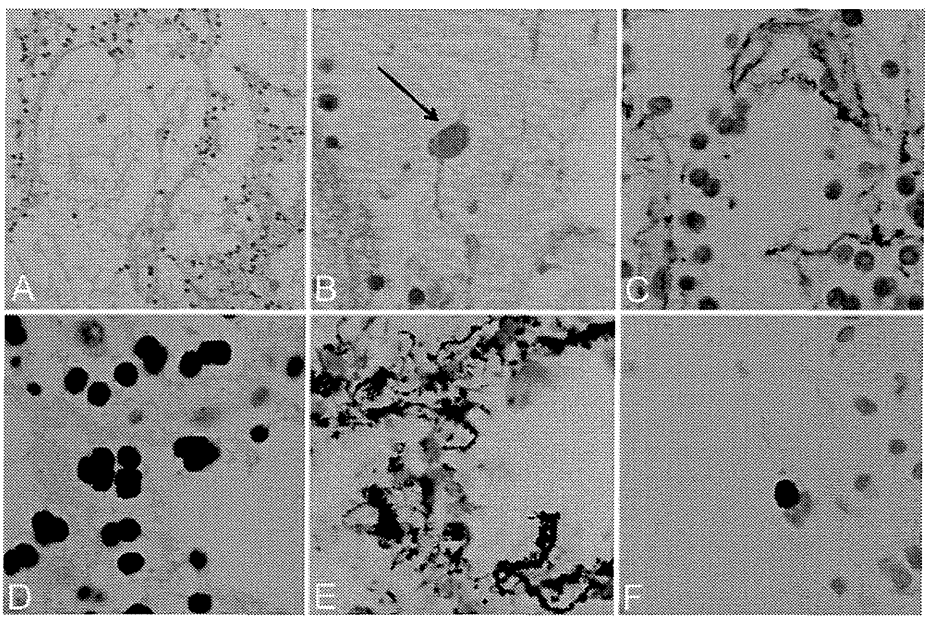

Fig. 5. Case 2. Photomicrographs of the second surgical specimen from the nonenhancing lesion in Fig. 4C. **A:** Glioneuronal elements in a columnar orientation are observed on a mucinous background. H & E, original magnification ×100. **B:** High-power view of A, showing floating neurons *(arrow)* scattered in the cystic structure. H & E stain, original magnification ×400. **C–E:** Immunostaining for GFAP (C), Olig2 (D), and NFP (E) were all positive. Original magnification ×400. **F:** The Ki 67 labeling index was 2%. Original magnification ×400.

The first documented case was reported by Hammond et al.,[8] who described malignant transformation of a DNET in a man who had undergone subtotal resection of a tumor without adjuvant therapy at the age of 29, after presenting with partial seizures. Eleven years later, he presented with progressive seizures. Magnetic resonance imaging revealed a "recurrent left midfrontal mass" with enhancement, and the patient underwent a second resection. The primary histological diagnosis at the first surgery was fibrillary astrocytoma, whereas the histological

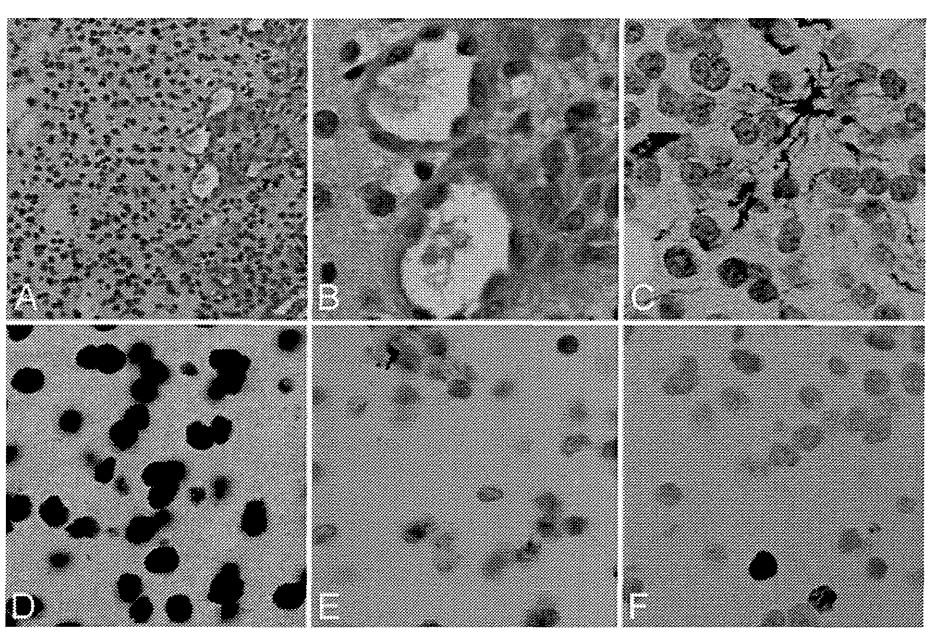

Fig. 6. Case 2. Photomicrographs of the second surgical specimen from the enhancing lesion. **A:** Oligodendroglia-like cells, and partly microvascular proliferation, are found with no apparent endothelial swelling. H & E stain, original magnification ×100. **B:** High-power view of A, showing no endothelial swelling and proliferation. H & E stain, original magnification ×400. **C–E:** Immunostaining for GFAP (C) and Olig2 (D) are positive, but NFP (E) is negative. Original magnification ×400. **F:** The Ki 67 labeling index was 2%. Original magnification ×400.

TABLE 2: Reported cases of malignant transformation of DNET*

Authors & Year	Age (yrs), Sex	Location	Interval (mos)	Recurrence/Progression			
				Enhancement	Resection	Histology	Ki 67 LI (%)
Hammond et al., 2000	29, M	frontal	132	+	subtotal	glioblastoma	35
Rushing et al., 2003	14, M	temporoparietal	36	+	subtotal	anaplastic astrocytoma†	12
Ray et al., 2009	12, F	parietal	80	+	subtotal	anaplastic astrocytoma†	8.5
present study, Case 1	4, F	frontoparietal	48	+	subtotal	anaplastic oligodendroglioma	30

* LI = labeling index.

† Initial histological diagnosis was low-grade glioma, and adjunctive radiotherapy was administered following initial surgical treatment.

diagnosis at the second surgery was Grade IV astrocytoma. The average Ki 67 labeling index of the specimen obtained during the second surgery was 35%. After the second surgery, the original specimen (from the first surgery) was reviewed and the diagnosis was revised to the complex form of DNET, based on the specific glioneuronal element feature of "floating neurons" and the oligodendroglia-like cells. In the first specimen, the random Ki 67 labeling index was 0.3% and the maximum Ki 67 index was 4%. The patient died 3 months after the second resection.

Rushing et al.[12] reported on a patient who first underwent subtotal resection of a tumor diagnosed as an oligoastrocytoma (histological diagnosis) at the age of 14 years. The Ki 67 labeling index was 0.1%–0.3%. The patient was treated with adjunctive radiation therapy consisting of 30 Gy to the whole brain followed by 25 Gy to the primary tumor site and subsequent oral lomustine (CCNU) chemotherapy. Three years after the initial resection, a recurrent lesion was found, with enhancement on CT. Another craniotomy was performed. The histological diagnosis was anaplastic astrocytoma, WHO Grade III. The Ki 67 labeling index was up to 12%. The original specimen was reviewed and some DNET features were identified. The Ki 67 labeling index was 0.1%–3.0% in the first specimen. The diagnosis of the original tumor was revised to the complex form of DNET.

Ray et al.[11] reported on a female patient who originally presented at the age of 12 years with left arm seizures and underwent subtotal resection at another hospital. The histological diagnosis was protoplasmic astrocytoma, WHO Grade II. Postoperatively, the patient underwent adjuvant radiation therapy (54 Gy). Seven years after the initial resection, an MRI study showed a lesion with ring enhancement, marked edema, and mass effect. The patient underwent subtotal resection of the lesion, followed by oral temozolomide administration. The histological diagnosis at the second surgery was anaplastic astrocytoma, WHO Grade III. The Ki 67 labeling index was up to 8.5%. Immunochemical staining showed a strong reaction for GFAP. Review of the first specimen identified oligodendroglia-like cells and numerous floating neurons and a Ki 67 labeling index of less than 1%. The revised histological diagnosis of the first specimen was DNET, WHO Grade I.

In the latter 2 cases of recurrent lesions, the patients were treated with radiation therapy after initial resection, and the potential mutagenic effects of radiation are known.[11,12] However, the first case, like our Case 1, involved malignant transformation of DNET without irradiation.[8] In addition, the patient in our Case 1 had an enhancing lesion that was found to be anaplastic oligodendroglioma within the typical DNET region, and the malignant transformation had occurred during the natural course of 4 years without resection.

These findings suggest that many DNETs may have been misdiagnosed as gliomas, and vice versa, in the past, resulting in needless radiochemotherapy or inadequate therapy, respectively. Refinement of the diagnostic criteria, especially for the complex and nonspecific forms of DNET, is essential to ensure correct and effective interventions.

Some DNETs show aggressive behavior, such as malignant transformation, but the prognostic factors for malignant transformation remain unknown. Recurrence is possible over 10 years after an initial resection, as shown by our Case 2. Close follow-up is required for patients with DNETs, especially when subtotal resection has been performed or the lesion is a complex DNET.

Genetic Background of DNETs

The genetic background of DNETs has not been systemically investigated. Neither loss of heterozygosity at 1p/19q or *TP53* gene mutation has been detected in DNETs,[7] nor has *IDH1* mutation.[2,9] The present 2 cases did not carry *IDH1/2* mutation and retained 1p and 19q, *TP53*, *PTEN*, *EGFR*, *CDKN2A*, and *ERBB2* in the nonenhancing tumor. These findings suggest that DNETs are genetically different from astrocytomas and oligodendrogliomas, which sometimes show a histological resemblance to the complex form of DNET. In one study of mutations in primary intracranial tumors, 60% of anaplastic oligodendrogliomas were found to have *IDH1* mutations,[9] so DNETs might be distinguished from astrocytomas and oligodendrogliomas based on the presence or absence of *IDH1/2* mutation. More genetic investigation of DNETs is required.

Conclusions

The present 2 unusual cases of DNETs occurred as recurrence with enhancement on MRI 10 years after initial resection, and the emergence of an enhancing lesion on MRI with malignant transformation during the natural

course of 4 years. Long-term follow-up is essential, even for the simple form of DNET and even after gross-total resection. If follow-up MRI reveals progressive behavior, resection should be performed without delay, with appropriate histological examination performed to identify aggressive subtypes of DNETs. Adjunctive radiochemotherapy is needed if the histological diagnosis demonstrates malignant transformation.

Disclosure

The authors report no conflict of interest concerning the materials or methods used in this study or the findings specified in this paper.

Author contributions to the study and manuscript preparation include the following. Conception and design: Kumabe. Acquisition of data: Kumabe, Mano, Shibahara, Saito, Sonoda, Watanabe. Analysis and interpretation of data: Kumabe, Mano, Shibahara, Saito, Sonoda, Watanabe. Drafting the article: Mano. Critically revising the article: all authors. Reviewed submitted version of manuscript: all authors. Approved the final version of the manuscript on behalf of all authors: Kumabe. Administrative/technical/material support: Shibahara, Sonoda. Study supervision: Kumabe, Tominaga.

References

1. Campos AR, Clusmann H, von Lehe M, Niehusmann P, Becker AJ, Schramm J, et al: Simple and complex dysembryoplastic neuroepithelial tumors (DNT) variants: clinical profile, MRI, and histopathology. **Neuroradiology 51:**433–443, 2009
2. Capper D, Reuss D, Schittenhelm J, Hartmann C, Bremer J, Sahm F, et al: Mutation-specific IDH1 antibody differentiates oligodendrogliomas and oligoastrocytomas from other brain tumors with oligodendroglioma-like morphology. **Acta Neuropathol 121:**241–252, 2011
3. Daumas-Duport C, Pietsch T, Hawkins C, Shankar SK: Dysembryoplastic neuroepithelial tumour, in Louis DN, Ohgaki H, Wiestler OD, et al (eds): **WHO Classification of Tumours of the Central Nervous System, ed 4.** Lyon: IARC Press, 2007, pp 99–102
4. Daumas-Duport C, Scheithauer BW, Chodkiewicz JP, Laws ER Jr, Vedrenne C: Dysembryoplastic neuroepithelial tumor: a surgically curable tumor of young patients with intractable partial seizures. Report of thirty-nine cases. **Neurosurgery 23:**545–556, 1988
5. Daumas-Duport C, Varlet P, Bacha S, Beuvon F, Cervera-Pierot P, Chodkiewicz JP: Dysembryoplastic neuroepithelial tumors: nonspecific histological forms—a study of 40 cases. **J Neurooncol 41:**267–280, 1999
6. Fernandez C, Girard N, Paz Paredes AP, Bouvier-Labit C, Lena G, Figarella-Branger D: The usefulness of MR imaging in the diagnosis of dysembryoplastic neuroepithelial tumor in children: a study of 14 cases. **AJNR Am J Neuroradiol 24:** 829–834, 2003
7. Fujisawa H, Marukawa K, Hasegawa M, Tohma Y, Hayashi Y, Uchiyama N, et al: Genetic differences between neurocytoma and dysembryoplastic neuroepithelial tumor and oligodendroglial tumors. **J Neurosurg 97:**1350–1355, 2002
8. Hammond RR, Duggal N, Woulfe JMJ, Girvin JP: Malignant transformation of a dysembryoplastic neuroepithelial tumor. Case report. **J Neurosurg 92:**722–725, 2000
9. Ichimura K, Pearson DM, Kocialkowski S, Bäcklund LM, Chan R, Jones DT, et al: IDH1 mutations are present in the majority of common adult gliomas but rare in primary glioblastomas. **Neuro Oncol 11:**341–347, 2009
10. Jensen RL, Caamano E, Jensen EM, Couldwell WT: Development of contrast enhancement after long-term observation of a dysembryoplastic neuroepithelial tumor. **J Neurooncol 78:** 59–62, 2006
11. Ray WZ, Blackburn SL, Casavilca-Zambrano S, Barrionuevo C, Orrego JE, Heinicke H, et al: Clinicopathologic features of recurrent dysembryoplastic neuroepithelial tumor and rare malignant transformation: a report of 5 cases and review of the literature. **J Neurooncol 94:**283–292, 2009
12. Rushing EJ, Thompson LD, Mena H: Malignant transformation of a dysembryoplastic neuroepithelial tumor after radiation and chemotherapy. **Ann Diagn Pathol 7:**240–244, 2003
13. Sampetrean O, Maehara T, Arai N, Nemoto T: Rapidly growing dysembryoplastic neuroepithelial tumor: case report. **Neurosurgery 59:**E1337–E1338, 2006
14. Schittenhelm J, Mittelbronn M, Wolff M, Truebenbach J, Will BE, Meyermann R, et al: Multifocal dysembryoplastic neuroepithelial tumor with signs of atypia after regrowth. **Neuropathology 27:**383–389, 2007
15. Shin JH, Lee HK, Khang SK, Kim DW, Jeong AK, Ahn KJ, et al: Neuronal tumors of the central nervous system: radiologic findings and pathologic correlation. **Radiographics 22:**1177–1189, 2002
16. Stanescu Cosson R, Varlet P, Beuvon F, Daumas Duport C, Devaux B, Chassoux F, et al: Dysembryoplastic neuroepithelial tumors: CT, MR findings and imaging follow-up: a study of 53 cases. **J Neuroradiol 28:**230–240, 2001

Manuscript submitted October 17, 2011.
Accepted January 15, 2013.
Please include this information when citing this paper: published online February 22, 2013; DOI: 10.3171/2013.1.PEDS11449.
Address correspondence to: Toshihiro Kumabe, M.D., Ph.D., Department of Neurosurgery, Tohoku University Graduate School of Medicine, 1-1 Seiryo-cho, Aoba-ku, Sendai-shi, Miyagi 980-8574, Japan. email: kuma@nsg.med.tohoku.ac.jp.

Acta Neuropathol (2013) 126:917–929
DOI 10.1007/s00401-013-1198-2

ORIGINAL PAPER

TERT promoter mutations are highly recurrent in SHH subgroup medulloblastoma

Marc Remke · Vijay Ramaswamy · John Peacock · David J. H. Shih · Christian Koelsche · Paul A. Northcott · Nadia Hill · Florence M. G. Cavalli · Marcel Kool · Xin Wang · Stephen C. Mack · Mark Barszczyk · A. Sorana Morrissy · Xiaochong Wu · Sameer Agnihotri · Betty Luu · David T. W. Jones · Livia Garzia · Adrian M. Dubuc · Nataliya Zhukova · Robert Vanner · Johan M. Kros · Pim J. French · Erwin G. Van Meir · Rajeev Vibhakar · Karel Zitterbart · Jennifer A. Chan · László Bognár · Almos Klekner · Boleslaw Lach · Shin Jung · Ali G. Saad · Linda M. Liau · Steffen Albrecht · Massimo Zollo · Michael K. Cooper · Reid C. Thompson · Oliver O. Delattre · Franck Bourdeaut · François F. Doz · Miklós Garami · Peter Hauser · Carlos G. Carlotti · Timothy E. Van Meter · Luca Massimi · Daniel Fults · Scott L. Pomeroy · Toshiro Kumabe · Young Shin Ra · Jeffrey R. Leonard · Samer K. Elbabaa · Jaume Mora · Joshua B. Rubin · Yoon-Jae Cho · Roger E. McLendon · Darell D. Bigner · Charles G. Eberhart · Maryam Fouladi · Robert J. Wechsler-Reya · Claudia C. Faria · Sidney E. Croul · Annie Huang · Eric Bouffet · Cynthia E. Hawkins · Peter B. Dirks · William A. Weiss · Ulrich Schüller · Ian F. Pollack · Stefan Rutkowski · David Meyronet · Anne Jouvet · Michelle Fèvre-Montange · Nada Jabado · Marta Perek-Polnik · Wieslawa A. Grajkowska · Seung-Ki Kim · James T. Rutka · David Malkin · Uri Tabori · Stefan M. Pfister · Andrey Korshunov · Andreas von Deimling · Michael D. Taylor

Received: 2 September 2013 / Accepted: 15 October 2013 / Published online: 31 October 2013

Abstract *Telomerase reverse transcriptase* (*TERT*) promoter mutations were recently shown to drive telomerase activity in various cancer types, including medulloblastoma. However, the clinical and biological implications of *TERT* mutations in medulloblastoma have not been described. Hence, we sought to describe these mutations and their impact in a subgroup-specific manner. We analyzed the *TERT* promoter by direct sequencing and genotyping in 466 medulloblastomas. The mutational distributions were determined according to subgroup affiliation, demographics, and clinical, prognostic, and molecular features. Integrated genomics approaches were used to identify specific somatic copy number alterations in *TERT* promoter-mutated and wild-type tumors. Overall, *TERT* promoter mutations were identified in 21 % of medulloblastomas. Strikingly, the highest frequencies of

Electronic supplementary material The online version of this article (doi:10.1007/s00401-013-1198-2) contains supplementary material, which is available to authorized users.

M. Remke · V. Ramaswamy · J. Peacock · D. J. H. Shih · N. Hill · F. M. G. Cavalli · X. Wang · S. C. Mack · M. Barszczyk · A. S. Morrissy · X. Wu · S. Agnihotri · B. Luu · L. Garzia · A. M. Dubuc · N. Zhukova · R. Vanner · M. D. Taylor
The Arthur and Sonia Labatt Brain Tumour Research Centre, The Hospital for Sick Children, Toronto, ON, Canada

M. Remke · V. Ramaswamy · J. Peacock · D. J. H. Shih · N. Hill · F. M. G. Cavalli · X. Wang · S. C. Mack · A. S. Morrissy · X. Wu · B. Luu · L. Garzia · A. M. Dubuc · M. D. Taylor
Developmental and Stem Cell Biology Program, The Hospital for Sick Children, Toronto, ON, Canada

M. Remke · V. Ramaswamy · J. Peacock · D. J. H. Shih · X. Wang · S. C. Mack · A. M. Dubuc · S. E. Croul · M. D. Taylor (✉)
Department of Laboratory Medicine and Pathobiology, University of Toronto, Toronto, ON, Canada
e-mail: mdtaylor@sickkids.ca

C. Koelsche · A. Korshunov · A. von Deimling (✉)
Department of Neuropathology, University Hospital Heidelberg, Heidelberg, Germany
e-mail: andreas.vondeimling@med.uni-heidelberg.de

C. Koelsche · A. Korshunov · A. von Deimling
Clinical Cooperation Unit Neuropathology, German Cancer Research Center (DKFZ), Heidelberg, Germany

P. A. Northcott · M. Kool · D. T. W. Jones · S. M. Pfister
Division of Pediatric Neurooncology, German Cancer Research Center (DKFZ), Heidelberg, Germany

J. M. Kros
Department of Pathology, Erasmus Medical Center, Rotterdam, The Netherlands

P. J. French
Department of Neurology, Erasmus Medical Center, Rotterdam, The Netherlands

TERT mutations were observed in SHH (83 %; 55/66) and WNT (31 %; 4/13) medulloblastomas derived from adult patients. Group 3 and Group 4 harbored this alteration in <5 % of cases and showed no association with increased patient age. The prognostic implications of these mutations were highly subgroup-specific. *TERT* mutations identified a subset with good and poor prognosis in SHH and Group 4 tumors, respectively. Monosomy 6 was mostly restricted to WNT tumors without *TERT* mutations. Hallmark SHH focal copy number aberrations and chromosome 10q deletion were mutually exclusive with *TERT* mutations within SHH tumors. *TERT* promoter mutations are the most common recurrent somatic point mutation in medulloblastoma, and are very highly enriched in adult SHH and WNT tumors. *TERT* mutations define a subset of SHH medulloblastoma with distinct demographics, cytogenetics, and outcomes.

Keywords TERT promoter mutations · SHH pathway · Adult · Medulloblastoma

Introduction

Medulloblastoma is a highly malignant embryonal brain tumor located in the posterior fossa [6, 29, 33, 35]. While this tumor comprises the most common malignant brain tumor in children, it only accounts for approximately 1 % of primary CNS tumors in adults [18, 20]. The current consensus recognizes four core molecular subgroups (WNT, SHH, Group 3, and Group 4) with distinct molecular, demographic, clinicopathological, and prognostic characteristics [5, 15, 16, 26, 27, 37, 38, 41, 42]. The defining features of medulloblastoma subgroups differ dramatically according to age at diagnosis [15, 27, 41]. Specifically, Group 3 tumors are largely confined to non-adults, SHH tumors are most frequent in infants and adults, while WNT and Group 4 medulloblastomas are mostly observed in pediatric cohorts [15, 24, 27, 38, 41]. Particularly within SHH tumors, age-associated heterogeneity was observed regarding the transcriptional characteristics, somatic copy number alterations (SCNA), and the prognostic implications of biomarkers [15, 18, 38, 40]. Delineation of tumorigenic features characteristic for these age-related

E. G. Van Meir
Departments of Neurosurgery and Hematology and Medical Oncology, School of Medicine and Winship Cancer Institute, Emory University, Atlanta, GA, USA

R. Vibhakar
Department of Pediatrics, University of Colorado Denver, Aurora, CO, USA

K. Zitterbart
Department of Pediatric Oncology, School of Medicine, Masaryk University and University Hospital Brno, Brno, Czech Republic

J. A. Chan
Department of Pathology and Laboratory Medicine, University of Calgary, Calgary, AB, Canada

L. Bognár · A. Klekner
Department of Neurosurgery, Medical and Health Science Centre, University of Debrecen, Debrecen, Hungary

B. Lach
Division of Anatomical Pathology, Department of Pathology and Molecular Medicine, McMaster University, Hamilton, ON, Canada

S. Jung
Department of Neurosurgery, Chonnam National University Research Institute of Medical Sciences, Chonnam National University Hwasun Hospital and Medical School, Chonnam, South Korea

A. G. Saad
Department of Pathology, University of Arkansas for Medical Sciences, Little Rock, AR, USA

L. M. Liau
Department of Neurosurgery, David Geffen School of Medicine at UCLA, Los Angeles, CA, USA

S. Albrecht
Department of Pathology, McGill University, Montreal, QC, Canada

M. Zollo
Dipartimento di Medicina Molecolare e Biotecnologie Mediche, University of Naples, Naples, Italy

M. Zollo
CEINGE Biotecnologie Avanzate, Naples, Italy

M. K. Cooper
Department of Neurology, Vanderbilt Medical Center, Nashville, TN, USA

R. C. Thompson
Department of Neurological Surgery, Vanderbilt Medical Center, Nashville, TN, USA

O. O. Delattre · F. Bourdeaut
Laboratoire de Génétique et Biologie des Cancers, Institut Curie, Paris, France

F. F. Doz
Department of Pediatric Oncology, Institut Curie and University Paris Descartes, Sorbonne Paris Cité, Paris, France

M. Garami · P. Hauser
2nd Department of Pediatrics, Semmelweis University, Budapest, Hungary

differences, particularly within SHH tumors, are highly desirable to understand these clear biological and prognostic discrepancies.

Telomere maintenance is fundamentally important to normal self-renewing stem cells and cancer cells [3, 7, 9, 14, 22]. It has been suggested that tumors derived from cell populations with low self-renewal capacity generally rely on alterations that restore telomerase activity, while epigenetic mechanisms maintain telomerase activity in tumor types derived from self-renewing stem cells [13]. The identification of recurrent *telomerase reverse transcriptase* (*TERT*) promoter mutations in 21 % of 91 medulloblastomas [13] is intriguing, since other mechanisms converging on increased telomerase activity including alternative lengthening of telomeres (ALT) [8] or mutations affecting the *ATRX/DAXX* complex are excessively uncommon in medulloblastoma [12, 25, 32, 34, 39]. Although *TERT* mutations have been reported in several cancers [2, 10, 11, 13, 19, 43], their putative association with distinct biological behavior and clinical or even prognostic characteristics has not been comprehensively studied. The initial analyses of *TERT* mutations in medulloblastoma [12] mainly catalogued the mutational frequency rather than correlating the molecular and clinical features of these mutations in a subgroup-specific manner.

In this study, we analyzed a representative set of 466 medulloblastomas for *TERT* promoter mutations. Subsequently, we correlated the mutational distribution with clinicopathological features, outcome, and molecular characteristics in a subgroup-specific manner. We demonstrate that *TERT* promoter mutations comprise the most recurrent mutation in adult SHH tumors identified to date and potentially define distinct prognostic subgroups in SHH and Group 4 medulloblastoma patients.

Materials and methods

Tumor material and patient characteristics

All tissues and clinicopathological information were serially collected in accordance with institutional review boards

C. G. Carlotti
Department of Surgery and Anatomy, Faculty of Medicine of Ribeirão Preto, Universidade de São Paulo, São Paulo, Brazil

T. E. Van Meter
Pediatric Hematology-Oncology, School of Medicine, Virginia Commonwealth University, Richmond, VA, USA

L. Massimi
Pediatric Neurosurgery, Catholic University Medical School, Rome, Italy

D. Fults
Department of Neurosurgery, Clinical Neurosciences Center, University of Utah, Salt Lake City, UT, USA

S. L. Pomeroy
Department of Neurology, Harvard Medical School, Children's Hospital Boston, Boston, ME, USA

T. Kumabe
Department of Neurosurgery, Tohoku University Graduate School of Medicine, Sendai, Japan

Y. S. Ra
Department of Neurosurgery, Asan Medical Center, University of Ulsan, Seoul, South Korea

J. R. Leonard
Division of Pediatric Neurosurgery, Department of Neurosurgery, Washington University School of Medicine, St. Louis Children's Hospital, St. Louis, MO, USA

S. K. Elbabaa
Division of Pediatric Neurosurgery, Department of Neurological Surgery, Saint Louis University School of Medicine, Saint Louis, MO, USA

J. Mora
Developmental Tumor Biology Laboratory, Hospital Sant Joan de Déu, Barcelona, Spain

J. B. Rubin
Departments of Pediatrics, Anatomy and Neurobiology, Washington University School of Medicine, St. Louis Children's Hospital, St. Louis, MO, USA

Y.-J. Cho
Department of Neurology and Neurological Sciences, Stanford University School of Medicine, Stanford, CA, USA

R. E. McLendon · D. D. Bigner
Department of Pathology, Duke University, Durham, NC, USA

C. G. Eberhart
Departments of Pathology, Ophthalmology and Oncology, John Hopkins University School of Medicine, Baltimore, MD, USA

M. Fouladi
Division of Oncology, Cincinnati Children's Hospital Medical Center, University of Cincinnati, Cincinnati, OH, USA

R. J. Wechsler-Reya
Sanford-Burnham Medical Research Institute, La Jolla, CA, USA

C. C. Faria · P. B. Dirks · J. T. Rutka · M. D. Taylor
Division of Neurosurgery, Department of Surgery, The Hospital for Sick Children and The Arthur and Sonia Labatt Brain Tumour Research Centre, Toronto, ON, Canada

C. C. Faria
Division of Neurosurgery, Hospital de Santa Maria, Centro Hospitalar Lisboa Norte EPE, Lisbon, Portugal

from various contributing centers to this study. Nucleic acid extractions were carried out as previously described [28]. The clinicopathological characteristics of the investigated patient cohort are outlined in Table 1. The median follow-up was 44.06 months (range 0.7–301.5 months).

Gene expression and copy number analysis

Subgroup affiliation was determined using nanoString limited gene expression profiling as previously described [31]. Somatic copy number alterations were assessed on the Affymetrix Single Nucleotide Polymorphism (SNP) 6.0 array platform in 418 of 466 cases to identify SCNAs specific for *TERT* mutant and wild-type tumors. Raw copy number estimates were obtained in dChip, followed by CBS segmentation in R as previously described [30]. Somatic copy number alterations were identified using GISTIC2 [21]. *TERT* expression levels were compared using R2 (www.r2.amc.nl). Differences in expression were tested using one-way ANOVA.

Sanger sequencing

Isolated DNA (25 ng) from all 466 tumors and 7 matched germline samples (25 ng) was amplified by PCR. PCRs contained 1 μl DNA template, 10 μM forward (5′-CAG GGC ACG CAC ACC AG-3′) and reverse (5′-GTC CTG CCC CTT CAC CTT C-3′) TERT-specific primers, and 12.5 μl HotStar Taq Plus Master Mix (Qiagen, Gaithersburg, Maryland, USA) in a 25 μl total reaction volume. Cycle parameters comprised 95 °C × 15 min; 28 cycles of 98 °C × 40 s, 65 °C × 30 s, 72 °C × 1 min; 72 °C × 10 min. PCRs were carried out using the C1000 Thermal Cycler (BioRad, Hercules, CA, USA). PCR products were purified with the PureLink PCR Micro kit (Life Technologies, Burlington, ON, Canada). In all experiments, controls were included in the absence of DNA to rule out contamination by PCR products. Templates for Sanger sequencing were analyzed with forward (5′-CAG CGC TGC CTG AAA CTC-3′) and reverse (5′-GTC CTG CCC CTT CAC CTT C-3′) sequencing primers using dGTP BigDye Terminator v3.0 Cycle Sequencing Ready Reaction Kit (Life Technologies), and 5 % DMSO on the ABI3730XL capillary genetic analyzer (Life Technologies).

Genotyping assay

Two primers (forward primer, 5′-CAG CGC TGC CTG AAA CTC-3′; reverse primer, 5′-GTC CTG CCC CTT CAC CTT C-3′) were designed to amplify a 163-bp product encompassing C228T and C250T hotspot mutations in the *TERT* promoter—corresponding to the positions 124 and 146 bp, respectively, upstream of the ATG start site. Two fluorogenic LNA probes were designed with different fluorescent dyes to allow single-tube genotyping. One probe was targeted to the WT sequence (*TERT*

A. Huang · E. Bouffet · D. Malkin · U. Tabori
Division of Haematology and Oncology, Department of Pediatrics, The Hospital for Sick Children, University of Toronto, Toronto, ON, Canada

C. E. Hawkins
Department of Pathology, The Hospital for Sick Children, Toronto, ON, Canada

W. A. Weiss
Department of Neurology, University of California, San Francisco, San Francisco, CA, USA

U. Schüller
Center for Neuropathology and Prion Research, University of Munich, Munich, Germany

I. F. Pollack
Department of Neurological Surgery, School of Medicine, University of Pittsburgh, Pittsburgh, PA, USA

S. Rutkowski
Department of Pediatric Hematology and Oncology, University Medical Center Hamburg-Eppendorf, Hamburg, Germany

D. Meyronet · A. Jouvet
Neuro-oncology and Neuro-inflammation Team, Inserm U1028, CNRS UMR 5292, Neuroscience Center, University Lyon 1, 69000 Lyon, France

D. Meyronet · A. Jouvet
Hospices Civils de Lyon, Centre de Pathologie et de Neuropathologie Est, Lyon 69003, France

M. Fèvre-Montange
Centre de Recherche en Neurosciences, INSERM U1028, CNRS UMR5292, Université de Lyon, Lyon, France

N. Jabado
Division of Experimental Medicine, McGill University, Montreal, QC, Canada

M. Perek-Polnik
Department of Oncology, The Children's Memorial Health Institute, Warsaw, Poland

W. A. Grajkowska
Department of Pathology, The Children's Memorial Health Institute, Warsaw, Poland

S.-K. Kim
Division of Pediatric Neurosurgery, Department of Neurosurgery, Seoul National University Children's Hospital, Seoul, Korea

S. M. Pfister
Department of Pediatric Oncology, Hematology, Immunology and Pulmonology, University Hospital Heidelberg, Heidelberg, Germany

Table 1 Clinicopathological and molecular characteristics according to *TERT* mutational status

Characteristic	*TERT* MUT	*TERT* WT	*p* value
Age (years)			
Median	22.00	7.08	**<0.0001**[#]
Range	0.66–49.00	0.24–56.32	
NA	1	0	
Gender			
Male	56	236	0.47[Φ]
Female	37	129	
NA	3	5	
Histology			
MBEN	3	8	0.59[χ]
Desmoplastic	10	59	
Classic	46	217	
LC/A	11	38	
NA	26	48	
M-stage			
M0	58	240	**0.03**[Φ]
M1-3	12	103	
NA	26	27	
TP53 status			
MUT	4	12	0.78[Φ]
WT	42	97	
NA	50	261	
Subgroup			
WNT	6	47	**<0.0001**[χ]
SHH	80	133	
Group 3	2	48	
Group 4	8	142	

F female, *LC/A* large cell/anaplastic, *M* male, *MB* medulloblastomal, *MBEN* medulloblastoma with extensive nodularity, *NA* not available (data were excluded from statistical comparison)

Bold values indicate $p < 0.05$

[#] Mann–Whitney *U* test

[Φ] Fisher's exact test

[χ] Chi-square test

WT, 5′-5HEX-CCC CTC CCG G-3IABkFQ-3′), and one was targeted to either of the two mutations (*TERT* mut, 5′-56FAM-CCC CTT CCG G-3IABkFQ). Primer and probes were custom designed by Integrated DNA Technologies (Coralville, Iowa, USA) using internal SNP design software, and sequence homogeneity was confirmed by comparison to all available sequences on the GenBank database using BLAST (http://www.ncbi.nlm.nih.gov/BLAST/). Primers were optimized to avoid for hairpins and homo- and heterodimers. Primers and probes were obtained from Integrated DNA Technologies.

Real-time PCR was performed in 25 μl reaction mixtures containing 12.5 μl of TaqMan Universal Master Mix II with UNG (Applied Biosystems), 900 nM concentrations of each primer, 250 nM *TERT* WT probe, 250 nM *TERT* MUT probe, and 1 μl (25 ng) of sample DNA. Thermocycling was performed on the StepOnePlus (Applied Biosystems) and consisted of 2 min at 50 °C, 10 min at 95 °C, and 40 cycles of 95 °C for 15 s and 60 °C for 1 min.

Analysis was performed using StepOne Software, version 2.1. Samples were considered mutant if they had CT values of ≤39 cycles. Each sample was verified visually by examining the PCR curves generated to eliminate false positives due to aberrant light emission. End-point allelic discrimination genotyping was performed by visually inspecting a plot of the fluorescence from the WT probe versus the MUT probe generated from the post-PCR fluorescence read.

Statistical analysis

Survival time according to *TERT* mutational status was assessed using the Kaplan–Meier estimate and a log-rank test. Comparisons of binary and categorical patient characteristics between subgroups and cohorts were performed using the two-sided Fisher's exact test or Chi-squared test. Continuous variables were analyzed using the Mann–Whitney *U* test. *p* values <0.05 were considered statistically significant. Multivariate Cox proportional hazards regression was used to adjust for additional covariates using the survival R package (v.2.36). All other statistical analyses were performed using StataSE 12 (Stata Corp. College Station, TX, USA) and Graphpad Prism 5 (La Jolla, CA, USA).

Results

Characteristics of *TERT*-mutated medulloblastomas

We performed Sanger sequencing on a clinically well-annotated medulloblastoma cohort ($n = 466$), reflecting the spectrum of demographics and histological subtypes of the disease (Table 1; Supplementary Figure 1A). Our results were verified using a Taqman-based genotyping assay that detects both of the most highly recurrent *TERT* promoter mutations (C228T and C250T). Since both mutational hotspots are located in highly homologous sequences, C228T and C250T mutations result in an identical binding sequence for the mutation-specific probe (CCCGGAAGGGG; Supplementary Figure 1B). A total of 21 % of medulloblastomas harbored *TERT* mutations (Fig. 1a). In line with a previous report, these mutations were enriched in older patients (Table 1; $p < 0.0001$), all mutations were heterozygous, and none of the available matched germline controls displayed this mutation [13]. Interestingly, we found that *TERT*-mutated medulloblastomas present less

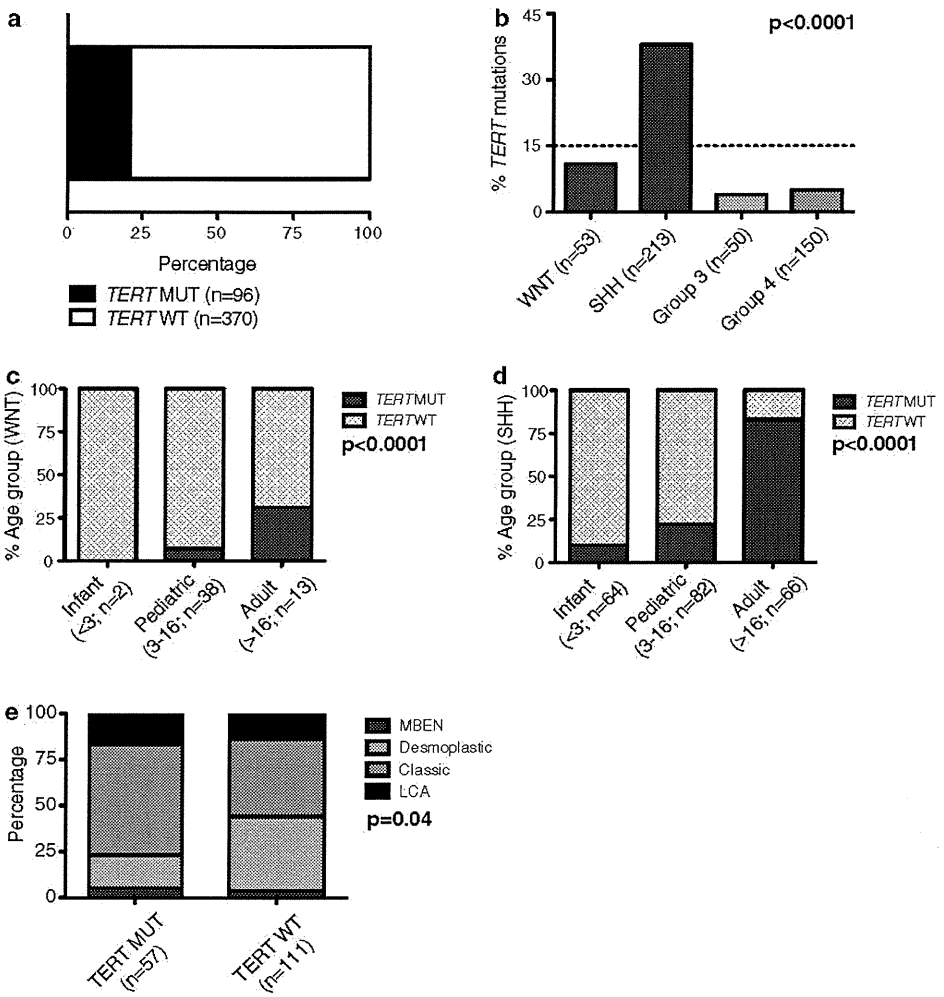

Fig. 1 *TERT* promoter-mutated medulloblastomas display distinct demographics, histology, and subgroup affiliation. **a** *Bar graph* indicating the frequency of *TERT* mutations in 466 primary medulloblastomas. **b** Prevalence of *TERT* mutations according to medulloblastoma subgroups, and within, **c** WNT and **d** SHH subgroups according to age groups. Distribution of histological variants within SHH tumors according to *TERT* mutational status (**e**). *MUT* mutation, *OS* overall survival, *WT* wild-type

frequently with metastatic dissemination at diagnosis compared to *TERT* wild-type tumors ($p = 0.03$).

TERT mutations are specifically enriched in SHH medulloblastomas

In a subgroup-specific analysis, we revealed that *TERT* mutations were significantly enriched in SHH tumors (80/213; 38 %; $p < 0.0001$) compared to WNT (6/53; 11 %) and Group 3 (2/50; 4 %) or Group 4 tumors (8/150; 5 %). *TERT* mutations in both WNT and SHH medulloblastomas were positively correlated with age. *TERT* mutations were significantly enriched in adult patients (Fig. 1c, d, both $p < 0.0001$). Increasing age was not associated with increased mutational frequency in either Group 3 or Group 4 tumors (n.s.). While histopathological features were similar between *TERT*-mutated and wild-type tumors across subgroups, we observed that classic histology was more commonly observed in *TERT* mutant SHH tumors, and desmoplastic histology in wild-type SHH tumors (Fig. 1e; Table 2; $p = 0.04$), respectively.

Prognostic implications of *TERT* mutations

When medulloblastoma patients across all subgroups were stratified by *TERT* mutational status, we observed no significant differences in survival (Fig. 2a; $p = 0.45$). Further after normalizing the subgroup composition to reported subgroup ratios, a statistical difference was still not revealed (data not shown; $p = 0.36$) [1, 15, 26, 41]. However, when *TERT* mutational status is re-analyzed in a subgroup-specific manner, several important survival associations are observed. *TERT* mutations had no prognostic impact within WNT tumors (Fig. 2b; $p = 0.17$). However, a significant association between *TERT* promoter mutations and outcomes was noted in SHH and Group 4 medulloblastomas. Specifically, the 5-year overall survival of SHH tumors with and without *TERT* mutations was 77.6 ± 7 %

Table 2 Clinicopathological and molecular characteristics of SHH medulloblastoma according to *TERT* mutational status

Characteristic	*TERT* MUT	*TERT* WT	*p* value
Age (years)			
Median	25.00	3.00	**<0.0001**[#]
Range	0.66–49.00	0.24–52.00	
NA	1	0	
Gender			
Male	46	80	0.77[Φ]
Female	31	48	
NA	3	5	
Histology			
MBEN	3	4	**0.04**[X]
Desmoplastic	10	44	
Classic	34	47	
LC/A	10	16	
NA	23	22	
M-stage			
M0	46	87	0.84[Φ]
M1-3	10	22	
NA	24	24	
TP53 status			
MUT	4	8	1[Φ]
WT	38	71	
NA	38	54	

F female, *LC/A* large cell/anaplastic, *M* male, *MB* medulloblastoma, *MBEN* medulloblastoma with extensive nodularity, *NA* not available (data were excluded from statistical comparison)

Bold values indicate $p < 0.05$

[#] Mann–Whitney *U* test

[Φ] Fisher's exact test

[X] Chi-square test

and 64.1 ± 5.1 %, respectively (Fig. 2c; $p = 0.04$). In contrast to the improved prognosis of *TERT* mutant SHH tumors, we observed the inverse pattern in Group 4 tumors where the 5-year overall survival for patients without and with *TERT* mutations was 73.3 % ± 4.3 % and 62.5 % ± 17.1 % (Fig. 2d; $p = 0.04$). Similar to the unfavorable prognosis of *TERT* mutations in Group 4 tumors, both of the patients with *TERT*-mutated Group 3 tumors died after 7 and 45 months of follow-up, respectively (Supplementary Table 1). Thus, we conclude that *TERT* mutations define distinct prognostic patient cohorts in a subgroup-specific fashion with good prognosis in SHH and poor prognosis in Group 4 medulloblastomas.

Survival analysis restricted to specific age groups

As *TERT* mutations are predominantly observed in non-infant medulloblastomas, we evaluated the prognostic implications of these promoter mutations across all four medulloblastoma subgroups in an age-dependent manner. *TERT* mutational status across subgroups had no prognostic impact among patients older than 3 years of age at diagnosis (Fig. 3a; $p = 0.59$). Interestingly, the prognostic impact of *TERT* mutation was more pronounced in the non-infant SHH population with a 5-year overall survival of 76.9 % ± 7.6 % and 59.3 % ± 6.9 % of non-infants with and without *TERT* promoter mutations, respectively (Fig. 3b; $p = 0.019$). These prognostic implications were similar in adult medulloblastoma patients and in the adult SHH subgroup (Supplementary Figure 2). In a subset of 76 SHH cases with known *TP53* mutational status [44], we revealed that *TP53* mutations identify non-infant SHH tumors with a particularly poor prognosis, while in contrast *TERT* mutations identify a subsets with good prognosis (Fig. 3c; $p = 0.047$). Mutations of both *TERT* and *TP53* were observed in 4/12 SHH tumors (Supplementary Table 2). Non-infant Group 4 showed an inverse prognostic association with poor outcome of *TERT*-mutated cases (Fig. 3d; $p = 0.024$). Lastly, we analyzed the overall survival of SHH patients under a multivariate Cox proportional hazards model comprising age at diagnosis, *TERT* mutational status, M-stage, and histology. In addition to the known prognostic significance of M-stage ($p < 0.001$) and histology ($p = 0.02$), we revealed that *TERT* status continued to be associated with good prognosis (HR 0.17, CI 0.04–0.69, $p = 0.01$), independent of other prognostic factors including age at diagnosis ($p = 0.35$).

Distinct somatic copy number alterations of *TERT*-mutated medulloblastomas

To identify additional genetic features associated with these distinct demographic and clinical differences, we evaluated broad and focal copy number alterations according to subgroup affiliation and *TERT* promoter mutations. Notably, only 1/6 (17 %) of *TERT*-mutated WNT tumors harbored monosomy 6, while this alteration is observed in approximately 80 % of *TERT* wild-type medulloblastomas of the WNT subgroup (Fig. 4a; $p = 0.005$). Loss of chromosome 2 and 10q loss were significantly enriched in *TERT* wild-type SHH tumors, while 3q loss was more frequently observed in their *TERT* mutant counterparts (Fig. 4b). Previously described focal alterations characteristic for SHH tumors including amplification of *MYCN/GLI2/CDK6/YAP1/PPM1D*, and deletions targeting *PTCH1/CDKN2A/CDKN2B/PTEN* were largely confined to *TERT* wild-type SHH medulloblastomas, while *TERT* mutant SHH (Fig. 5) and Group 4 (Supplementary Figure 3) showed very few focal SCNAs. Consistent with the higher frequency of *TERT* mutations in SHH tumors, we observed increased *TERT* expression in the SHH subgroup compared to Group

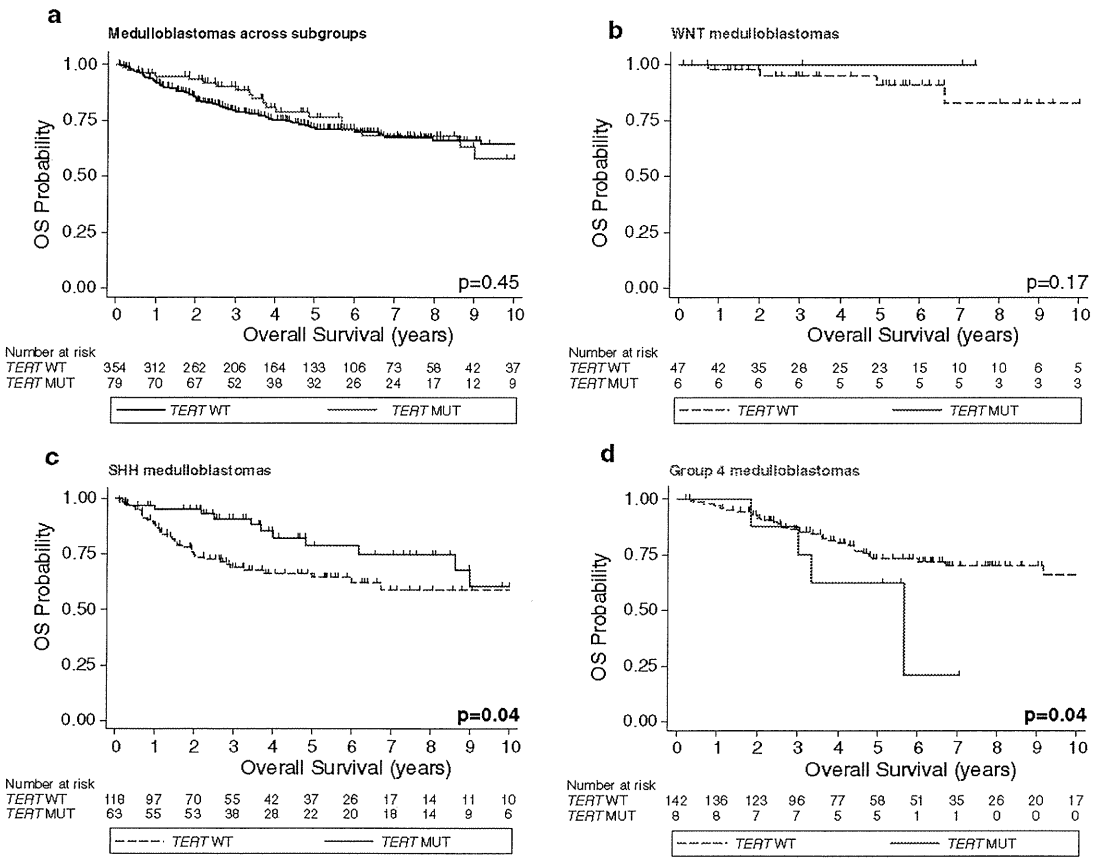

Fig. 2 Prognostic impact of *TERT* promoter mutations varies according to medulloblastoma subgroups. Kaplan–Meier estimate displaying overall survival (OS) according to *TERT* mutational status in primary medulloblastomas (**a**), within WNT (**b**), SHH (**c**), and Group 4 (**d**) subgroups. Survival differences were calculated using continuous log-rank tests. *MUT* mutation, *OS* overall survival, *WT* wild-type

4 tumors in two independent gene expression profiling studies ($p < 0.001$; Supplementary Figure 4). Furthermore, we observed *TERT* amplification in two tumors included in the entire cohort of 1,088 previously studied tumors [30]. Both of these cases with *TERT* amplification were SHH-driven medulloblastomas with wild-type *TERT* status, which were derived from pediatric patients who were both alive after 15 and 83 months of follow-up (Supplementary Figure 5). Thus, broad and focal SCNAs underline that *TERT* mutations define a genetically distinct subset within SHH tumors and possibly within the WNT and Group 4 tumors.

Discussion

The underlying biology of adult medulloblastomas remains poorly understood. Next-generation sequencing studies have revealed a broad spectrum of novel, potentially tumorigenic mutations in the recent past, but none of these studies focused on adult medulloblastomas [12, 25, 32, 34, 39]. In addition, the vast majority of these mutations are not recurrent enough to stratify patients into distinct clinical and prognostic subgroups.

In this study, we demonstrate that *TERT* promoter mutations, initially described in melanoma [10, 11], comprise the most recurrent mutation described so far across medulloblastoma subgroups, with a particular enrichment in older patient cohorts. These somatic mutations are especially common in older patients with SHH tumors (83 %) and to a lesser extent in adults with WNT medulloblastomas (11 %). Based on the transcriptional heterogeneity of SHH tumors in infant and adult patients, we suspect that the adult cluster mainly comprised *TERT*-mutated medulloblastomas [24]. According to the initial classification of tumor types with *TERT* mutations at frequencies over 15 % (*TERT*-high) vs. below this threshold (*TERT*-low) [13], our report suggests distinct baseline telomerase activity of the cell of origin in each of the subgroups (Group 3 ≥ Group 4 > WNT >> SHH). Furthermore, the identification of